MOLECULAR AND CELLULAR BIOLOGY, Nov. 2004, p. 9295–9304 Vol. 24, No. 21
0270-7306/04/$08.00+0 DOI: 10.1128/MCB.24.21.9295–9304.2004

Conditional Activation of Akt in Adult Skeletal Muscle Induces Rapid Hypertrophy

Ka-Man V. Lai, Michael Gonzalez, William T. Poueymirou, William O. Kline, Erqian Na, Elizabeth Zlotchenko, Trevor N. Stitt, Aris N. Economides, George D. Yancopoulos, and David J. Glass*

Regeneron Pharmaceuticals, Inc., Tarrytown, New York

Received 14 June 2004/Accepted 2 August 2004

Skeletal muscle atrophy is a severe morbidity caused by a variety of conditions, including cachexia, cancer, AIDS, prolonged bedrest, and diabetes. One strategy in the treatment of atrophy is to induce the pathways normally leading to skeletal muscle hypertrophy. The pathways that are sufficient to induce hypertrophy in skeletal muscle have been the subject of some controversy. We describe here the use of a novel method to produce a transgenic mouse in which a constitutively active form of Akt can be inducibly expressed in adult skeletal muscle and thereby demonstrate that acute activation of Akt is sufficient to induce rapid and significant skeletal muscle hypertrophy in vivo, accompanied by activation of the downstream Akt/p70S6 kinase protein synthesis pathway. Upon induction of Akt in skeletal muscle, there was also a significant decrease in adipose tissue. These findings suggest that pharmacologic approaches directed toward activating Akt will be useful in inducing skeletal muscle hypertrophy and that an increase in lean muscle mass is sufficient to decrease fat storage.

Skeletal muscle mass is increased in response to positive changes in workload or activity as a result of hypertrophy of individual muscle fibers, but the key molecular mediators of hypertrophy are only beginning to be elucidated (10). Induction of hypertrophy in adult skeletal muscle is accompanied by the increased expression of insulin-like growth factor 1 (IGF-1) (7, 11). When IGF-1 levels were enhanced by using a muscle-specific promoter in transgenic mice, increased muscle size resulted (4, 13). Also, the addition of IGF-1 in vitro to differentiated muscle cells promotes myotube hypertrophy (9, 18, 19), supporting the idea that hypertrophy can be mediated by pathways activated by autocrine or paracrine sources of IGF-1.

The binding of IGF-1 to its receptor triggers the activation of several intracellular kinases, including phosphatidylinositol-3-kinase (PI3K). PI3K phosphorylates the membrane phospholipid phosphatidylinositol-4,5-bisphosphate, creating a lipid-binding site on the cell membrane for a serine/threonine kinase called Akt (also called Akt1 or protein kinase B). Cell growth and survival in a variety of tissues and cell types in response to IGF-1, insulin, and other growth factors is mediated by Akt (6, 23). Direct and indirect targets downstream of Akt include glycogen synthase kinase 3, the mammalian target of rapamycin (mTOR), $p70^{S6K}$, and PHAS-1 (4EBP-1), key regulatory proteins involved in translation and protein synthesis (5, 14, 20). Indeed, induction of protein synthesis seems to be a key mechanism for inducing muscle fiber hypertrophy (10).

During adaptive hypertrophy in adult muscle and in IGF-1-induced myotube hypertrophy, Akt is phosphorylated and activated (2). Genetic approaches have provided further evidence for the role of the PI3K/Akt pathway in hypertrophy. Expression of constructs, via electroporation, encoding constitutively active forms of either PI3K or Akt induced muscle fiber hypertrophy both in vivo (2, 16) and in vitro (18, 19). Mice in which Akt has been genetically disrupted display growth defects (3), and those in which Akt and a related gene, Akt2, are both disrupted undergo skeletal muscle atrophy (17). However, to date, transgenic animals have not been produced expressing constitutively active Akt (c.a.Akt) in skeletal muscle, nor has Akt been conditionally activated in the adult animal, as a way to test whether its activation is sufficient to induce hypertrophy. We describe here the production of such transgenic animals and demonstrate a novel method for inducing conditional transgenic tissue-specific expression in an adult animal.

MATERIALS AND METHODS

Construction of targeting vectors and generation of chimeric mice. The muscle-specific constitutive Akt-EGFP (caAkt.EGFP) transgenic targeting vector was constructed by inserting at the NheI site of a 12.3-kb *ROSA-26* genomic fragment with sequences of a promoterless neo^R, three copies of poly(A) sequence, followed by the human skeletal actin (HSA) promoter and a cDNA of constitutive active Akt fused with enhanced green fluorescent protein (EGFP) (18). NotI-linearized targeting vector (30 μg) was electroporated into R1 embryonic stem (ES) cells as described previously (22). The frequency of homologous recombination was ~80%. Chimeric mice were generated by injection of targeted ES clones into C57BL/6 blastocysts. Male chimeras were mated with C57BL/6 females to generate F_1 heterozygote mice for all experiments.

Southern blotting and by PCR. Genomic DNA prepared from tail biopsies or muscles was subjected to Southern blot and/or PCR analysis as described previously (1). Briefly, 5 μg of AvrII-digested genomic DNA was hybridized to a ROSA-26 probe to detect a 5.3-kb restriction fragment from the wild type (WT), along with a 8.7-kb fragment from the $Akt^{Ind.\ Tg}$ mice. Tamoxifen-induced DNA recombination was characterized by using a EGFP probe to detect a 7.5- and 4.2-kb restriction fragments from the unrearranged and CreER (Cre fused to the estrogen receptor) deletion alleles, respectively. The amount of DNA recombination detected on the Southern blot was quantified by densitometry.

The rearranged allele was independently assayed by a PCR cycled 22 times (30 s at 94°C, 30 s at 60°C, and 2.5 min at 72°C), which amplified a 474-bp fragment of the heterozygous allele and a 254-bp fragment of the rearranged allele. We

* Corresponding author. Mailing address: Regeneron Pharmaceuticals, Inc., 777 Old Saw Mill River Rd., Tarrytown, NY 10591-6707. Phone: (914) 345-7527. Fax: (914) 345-7650. E-mail: david.glass@regeneron.com.

used the oligonucleotides 5′-F (5′-CGG ACA TTA ACC TAG GTC TGA AG-3′) corresponding to the region 5′ to the first LoxP sequence, Cre-R (5′-GAT CCG CCG CAT AAC CAG T-3′) corresponding to the CreER cassette, and 3′-R (5′-CTC TAG ACT TGG GCT TGC TCT-3′) matching sequences 3′ to the second LoxP site (see Fig. 2A).

RNA preparation and Northern blot analysis. Total RNA from individually genotyped muscle was isolated by using the Mixer Mill MM 300 (Qiagen) and the TRI reagent protocol (MRC, Inc.). First, 10 μg of total RNA was used per sample and run on a 1% formamide agarose gel, transferred to a Magna nylon transfer membrane (Osmonics), UV cross-linked, and stained with methylene blue. Hybridization was performed as described for Southern blotting except that the washing was carried out with 2× SSC (1× SSC is 0.15 M NaCl plus 0.015 M sodium citrate)–0.1% sodium dodecyl sulfate solution and the setup for exposure was with Kodak X-Omat Blue film at −80°C. [^{32}P]dCTP-labeled EGFP probe (to detect the ~3-kb *caAkt.EGFP* transcript) was synthesized by using a Prime-It random primer labeling kit (Stratagene) and purified by using the ProbeQuant G-50 Micro Columns (Amersham Pharmacia Biotech).

Tamoxifen administration and experimental procedures. For tamoxifen administration, 6- to 8-week-old mice were injected intraperitoneally daily for 7 or 14 consecutive days with 1 mg of tamoxifen dissolved in corn oil. At the completion of the experiment (1 day or 7 days after the final injection), the mice were euthanized with CO_2, followed by cervical dislocation. The tibialis anterior (TA) and gastrocnemius (GA) muscles were removed and weighed. All collected muscles and organs were frozen and were kept at −80C for future examination. All animal procedures were conducted in compliance with protocols approved by the Institutional Animal Care and Use Committee.

Immunohistochemical analysis. Histological analysis of the isopentane-frozen TA and GA muscles was performed as described previously (1). For double immunohistochemical labeling of cross-sections of the GA muscles with anti-laminin antibody (Sigma) at 1:2,000 and with anti-GFP polyclonal antibody (Chemicon) at 1:500, 10- to 15-μm cryostat sections were fixed in 4% paraformaldehyde and blocked with 10% normal goat serum and 0.2% Triton X-100 in phosphate-buffered saline (PBS). After incubation with primary antibodies overnight at 4°C in a humidified chamber, the slides were washed and then treated with secondary antibodies of Alexa Fluor 594-labeled anti-rabbit immunoglobulin G (IgG) anti-chicken IgG (Molecular Probes) at 1:200 and fluorescein-labeled anti-rabbit IgG (Molecular Probes) at 1:500. Sections were subsequently washed, labeled with Hoechst no. 33258 (Sigma) at 1 μg/ml, mounted, and analyzed by using a Nikon (Eclipse TE300) microscope equipped with appropriate filters and a ×20 objective lens.

Evaluation of single muscle fibers by confocal microscopic imaging. Preparation and staining of muscle fibers was performed as described previously (17a). Briefly, the quadriceps muscle was excised, fixed at 4C overnight in 4% paraformaldehyde, and washed in PBS. Bundles of individual muscle fibers were teased and mounted for fluorescent observation. For immunolabeling with anti-α-actinin antibody (Sigma) at 1:1,000, the teased fibers were blocked with 0.1% bovine serum albumin–0.4% Triton X-100–5% goat serum in PBS, incubated with primary antibody overnight, washed extensively, and detected with secondary antibody of Cy3-labeled goat anti-mouse IgG (Sigma) at 1:500 before being mounted in Vectashield (Vector Laboratories) for imaging. Immunostained and EGFP expressing teased muscle fibers were analyzed by confocal microscopy (Leica TCS SPII system). Images were magnified at ×40, ×80, or ×160 and are the single-plane projections of confocal stacks of images.

Protein preparation and Western blotting. Individual tissues samples were homogenized on ice in buffer A (1% NP-40 buffer, 50 mM HEPES [pH 7.4], 150 mM NaCl, 1 mM EDTA, 30 mM sodium pyrophosphate, 50 mM NaF, 1 mM sodium orthovanadate, 10 μg of aprotinin/ml, 10 μg of leupeptin/ml, 5 mM benzamidine, 1 mM phenylmethylsulfonyl fluoride, 5 mM *N*-ethylmaleimide, 25 mM β-glycerophosphate, 100 nM okadaic acid, 5 nM microcystin LR) and centrifuged for 20 min at 14,000 × *g*. The supernatant was taken, and the protein level was quantified (BCA Protein Assay; Pierce, Rutherford, Ill.). Equal amounts of protein were resolved by sodium dodecyl sulfate-polyacrylamide gel electrophoresis (8% precast gels; Novex) and immunoblotted with Akt or phospho-specific Akt (S^{473}) polyclonal antibodies (New England BioLabs) at 1:1,000. After secondary antibody incubation (horseradish peroxidase-conjugated goat anti-rabbit antibody), signal was detected by an enhanced chemiluminescence detection system (Renaissance; Dupont-NEN). The detection of p70S6K was performed as reported elsewhere (18).

Statistical analysis. Muscle fiber size was obtained from digitally imaged serial cross-sections of cryostat-sectioned muscle. Individual muscle fibers were outlined, and the cross-sectional areas were determined by using a computer-assisted image analysis system (MetaMorph; Universal Imaging Corp.). All data are expressed as means ± the standard error of the mean (represented as error bars). Analysis of variance was conducted by using the program Statview and Fisher post hoc correction for multiple paired comparisons was used for comparisons between groups. Statistical significance was set at a P value of <0.05.

RESULTS

To examine the role of Akt in in vivo hypertrophy, a variation of the traditional transgenic mouse was utilized, in which a single copy of c.a.Akt that was fused to EGFP as a marker was engineered to be expressed via the HSA promoter. This HSA-c.a.Akt-EGFP cassette was recombined into the *ROSA-26* locus (24) via targeted insertion by homologous recombination (Fig. 1A).

Several transgenic HSA-c.a.Akt-EGFP (Akt^{Tg}) chimeric animals, which arose from mixing ES cells containing the recombined transgene with WT ES cells, lived to maturity and underwent profound skeletal muscle hypertrophy (Fig. 1B), demonstrating that expression of c.a.Akt throughout development is sufficient to induce a significant increase in skeletal muscle mass. In order to determine whether the increase in muscle size was a result of actual myofiber hypertrophy, a cross-section of skeletal muscle obtained from the Akt^{Tg} chimera was compared to WT muscle (Fig. 1D): a >2-fold increase in average diameters was observed in TA muscle (Fig. 1E, WT control [739 ± 2 μm^2] versus Akt^{Tg} chimera [1,770 ± 41 μm^2]), and a 1.5-fold increase was seen in the medial gastrocnemius (MG) (Fig. 1E, WT control [2,023 ± 0 μm^2] versus

FIG. 1. Constitutive activation of Akt in transgenic chimeras (Akt^{Tg}) results in skeletal muscle hypertrophy. (A) Strategy for generation of Akt^{Tg} animals. A partial map of the WT mouse *ROSA-26* locus, including exon 2 (E2) is shown. Upon homologous recombination, the targeting vector inserted a total of 7.4 kb—including a neomycin resistance cassette (NEO), the HSA promoter, and a constitutively active form of Akt fused to EGFP (c.a.Akt-EGFP)—into the *ROSA-26* locus. WT and targeted loci are shown. Abbreviations: A, AvrII; B, BamHI; RV, EcoRV; N, NotI. (B) Akt^{Tg} chimeras displayed a hypertrophic skeletal muscle phenotype. Increased skeletal muscle size is evident when we compared an Akt^{Tg} animal to a WT littermate. Double-headed arrows point to a muscle that is significantly larger in the Akt^{Tg}. The single arrow points to a fat pad in the WT that is absent in the Akt^{Tg} chimeric animals. (C) The transgenic c.a.Akt-EGFP fusion protein is phosphorylated and is expressed at high levels in skeletal muscle in an immunoblot of total protein lysates isolated from Akt^{Tg} and WT muscles. Both endogenous Akt and the c.a.Akt-EGFP fusion protein are evident in muscle from the Akt^{Tg}, whereas only endogenous Akt is seen in muscle from the WT animal (top panel). The c.a.Akt-EGFP protein is phosphorylated on Serine-473. In the WT animal, only muscle obtained from a CH model is phosphorylated (bottom panel). Lanes (muscle abbreviations): BW, abdominal body wall; TA, tibialis anterior; GA, gastrocnemius; Quad, quadriceps; PL, plantaris. (D) Transverse sections of muscles immunostained with an anti-laminin antibody to outline the perimeters of muscle fibers. Enlarged fibers are evident in both TA and MG (medial gastrocnemius) muscles of Akt^{Tg} but not in the WT. (E) Mean cross-sectional area of muscle fibers. TA and MG muscle fibers are significantly (✻) larger in the Akt^{Tg} compared to WT. Significance assessed by using the Student t test ($P < 0.05$). (F) Distribution of mean cross-sectional areas of muscle fibers. Individual TA and MG muscle fiber sizes from the Akt^{Tg} (red bars) are shifted to the right side of the curve in comparison to those from the WT (gray bars).

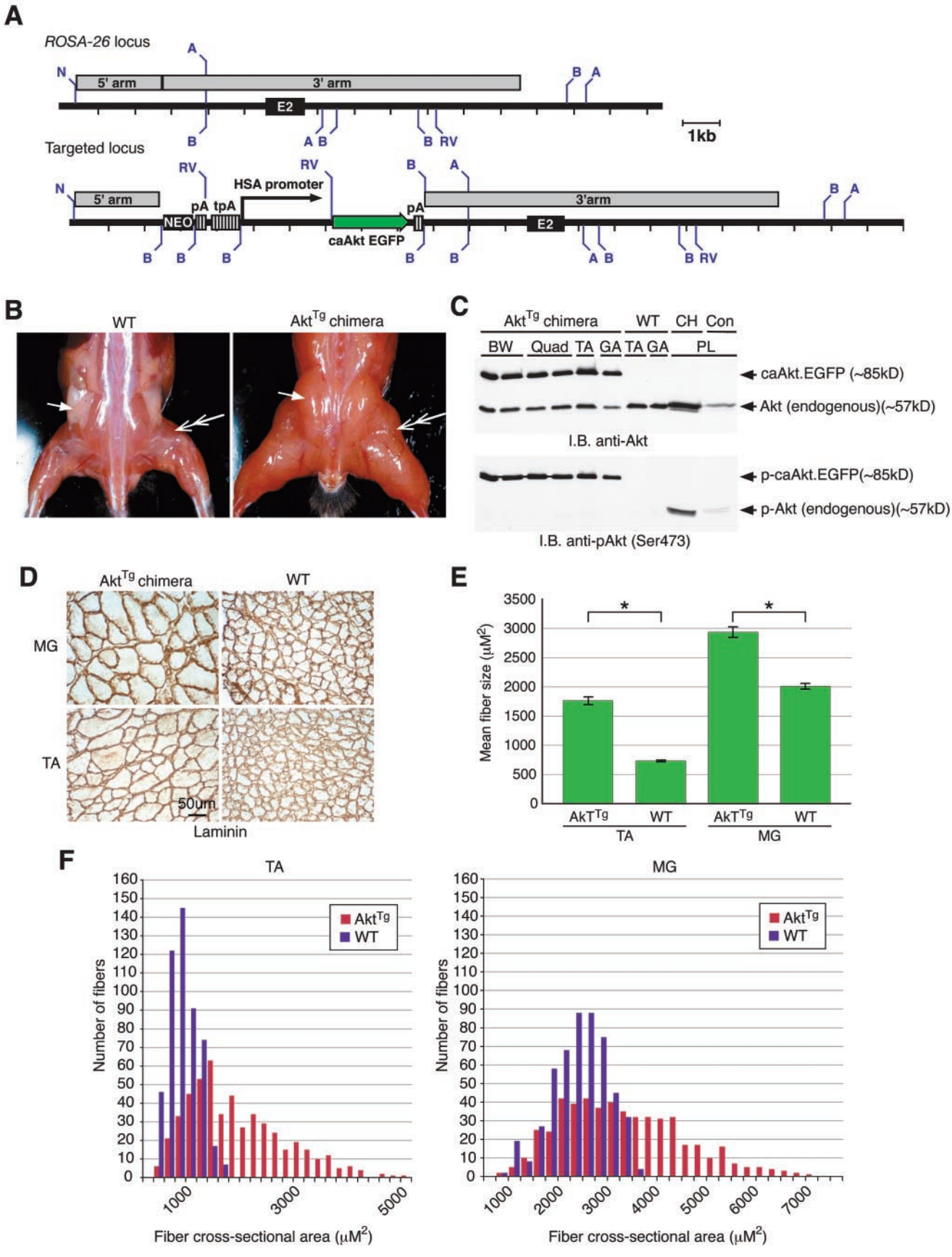
A
ROSA-26 locus
N
5' arm
3' arm
E2
A
B
B A
A B
B RV
1kb
Targeted locus
RV
HSA promoter
pA tpA
NEO
caAkt EGFP
pA
3'arm
B
RV
B
A
B
B
B
B
B
A B
B RV
B
WT
Akt^Tg chimera
C
Akt^Tg chimera
WT
CH
Con
BW
Quad
TA
GA
TA
GA
PL
caAkt.EGFP (~85kD)
Akt (endogenous)(~57kD)
I.B. anti-Akt
p-caAkt.EGFP(~85kD)
p-Akt (endogenous)(~57kD)
I.B. anti-pAkt (Ser473)
D
Akt^Tg chimera
WT
MG
TA
50um
Laminin
E
Mean fiber size (μM²)
3500
3000
2500
2000
1500
1000
500
0
*
*
AkT^Tg
WT
AkT^Tg
WT
TA
MG
F
TA
MG
Akt^Tg
WT
Number of fibers
160
150
140
130
120
110
100
90
80
70
60
50
40
30
20
10
0
1000
3000
5000
2000
4000
6000
7000
Fiber cross-sectional area (μM²)

Akt^{Tg} chimera [2,943 ± 61 μm^2]). An analysis of the individual fiber sizes demonstrates a significant shift to the right in TA and MG Akt^{Tg} muscles (Fig. 1F).

Of interest, chimeric expression of c.a.Akt-EGFP in skeletal muscle results in animals with little or no body fat (Fig. 1B, single arrows), despite a lack of expression of the transgene in adipose tissue (data not shown).

We next analyzed the expression levels of the transgenic c.a.Akt-EGFP fusion protein and its activation state in the muscles of Akt^{Tg} animals. Using an antibody specific for Akt, we found that a unique protein was recognized in muscle obtained from the Akt^{Tg} chimeric animals, a finding consistent with the predicted size for the c.a.Akt-EGFP fusion protein (85 kDa) (Fig. 1C). This same antibody also recognized endogenous Akt in both the chimeric animals and the WT control animals (Fig. 1C). To determine whether Akt was activated in the chimeras, an antibody was used which binds to a phosphorylation site on Akt (Ser-473), which denotes Akt activation. Immunoblotting with this phospho-specific Akt antibody demonstrated that the c.a.Akt-EGFP fusion molecule was indeed active in all muscles analyzed (Fig. 1C); the level of activation was compared, as a positive control, to endogenous Akt expressed in plantaris muscle undergoing compensatory hypertrophy (CH) (Fig. 1C). In a prior study it had been demonstrated that Akt is activated during skeletal muscle hypertrophy (2). Unfortunately, we were not able to breed the Akt^{Tg} chimeric animals to heterozygosity, probably due to lethal embryonic cardiac expression that was observed in many of the chimeric embryos examined (data not shown).

Although the data obtained from the chimeras was suggestive, we were interested in obtaining true c.a.Akt transgenics and were further curious to know whether the effects we were seeing were a function of long-term developmental changes that occurred as a result of activation of Akt throughout embryogenesis, or whether acute activation of Akt in adult skeletal muscle was sufficient to cause hypertrophy. We therefore progressed to a second, novel method designed to induce expression of c.a.Akt in skeletal muscle.

First, we took advantage of the tamoxifen-dependent CreERt2 to induce transgene expression (8). Others have shown that conditional expression of a transgene can be induced by using this system, which takes advantage of the bacterial Cre recombinase, fused to a mutated estrogen receptor (i.e., CreERt2) (8). We obviated the need for a mating, and the potential complications that may arise due to multiple unknown integration sites, by recombining the HSA-driven CreERt2 transgene in cis with the c.a.Akt-EGFP cassette into a known locus: the *ROSA-26* locus (Fig. 2A). Using this approach, prior to the addition of tamoxifen, the HSA promoter drives transcription of CreERt2, whereas transcription of *c.a.Akt-EGFP* is largely absent. After the addition of tamoxifen, the CreERt2 cassette drives its own excision, recombining the c.a.Akt-EGFP cassette downstream of the HSA promoter (Fig. 2A). Since the deletion of the CreERt2 cassette is permanent, HSA-driven transcription of *c.a.Akt-EGFP* will continue even after the withdrawal of tamoxifen. With this system we were able to produce heterozygotic transgenic animals, called $Akt^{Ind.Tg}$. Southern analysis of $Akt^{Ind.Tg}$ genomic DNA demonstrated that heterozygotic animals contained the cassettes in the *ROSA-26* locus (Fig. 2B) and that, after treatment with tamoxifen, 10 to 32% of the loci underwent recombination, depending on the muscle tested (Fig. 2C). The Southern data was confirmed by a semiquantitative PCR assay, designed to distinguish between the unrearranged targeted allele and the tamoxifen-dependent CreERt2-mediated recombined caAkt-EGFP cassette at the ROSA locus (Fig. 2D). The recombination is evident in skeletal muscle DNA but not in tail DNA (Fig. 2C and D).

WT and $Akt^{Ind.Tg}$ animals were injected daily with tamoxifen for 2 weeks and analyzed after an additional week after tamoxifen treatment. This short-term induction of the *c.a.Akt-EGFP* transgene resulted in a significant increase in the size of skeletal muscle (Fig. 2E), as quantified by measuring differences in mean weight between untreated and tamoxifen-treated WT and $Akt^{Ind.Tg}$ mice (Fig. 2F). The analysis showed that both male and female tamoxifen-treated $Akt^{Ind.Tg}$ animals experienced statistically significant increases in muscle weight compared to untreated WT and $Akt^{Ind.Tg}$ animals and tamoxifen-treated WT control animals (Fig. 2F). Coincident with the increase in muscle mass was a loss of visible adipose tissue deposits (Fig. 2E).

To directly evaluate the morphology of the muscles in the

FIG. 2. Postnatal induction of muscle-specific c.a.Akt-EGFP ($Akt^{Ind.Tg}$) expression in transgenic mice results in rapid skeletal muscle hypertrophy. (A) Strategy for the generation of $Akt^{Ind.Tg}$ animals. The tamoxifen-inducible HSA.CreERt2.$Akt^{Ind.Tg}$ targeting cassette is generated by inserting a floxed Cre-ERt2 and stop sequence 5′ to c.a.Akt-EGFP of the HSA-c.a.Akt-EGFP transgenic construct (Fig. 1A). Upon homologous recombination, the new targeting vector inserted a total of 11 kb into the *ROSA-26* locus (targeted locus). Tamoxifen induces the excision of the floxed Cre-ERt2 cassette. The c.a.Akt-EGFP cassette is transcribed by the HSA promoter as a result of DNA recombination (recombined locus). (B) Southern analysis of targeted *ROSA-26* locus. Genotyping of AvrII-digested genomic DNA by Southern blot hybridization with a probe specific to the *ROSA-26* locus. Arrows indicate the 5.3-kb WT fragment and the 8.7-kb targeted $Akt^{Ind.Tg}$ allele. (C) Determination of tamoxifen-induced recombination of the $Akt^{Ind.Tg}$ allele by Southern blot analysis. An EGFP probe was used to distinguish the 4.2-kb recombined $Akt^{Ind.Tg}$ allele from the 7.5-kb targeted *ROSA-26* allele from AvrII-digested genomic DNA. Recombination was only detected in DNA isolated from tamoxifen-treated muscles of $Akt^{Ind.Tg}$ mice. Lanes (muscle abbreviations): TA, tibialis anterior; GA, gastrocnemius; Quad, quadriceps. An arrow points to the 4.2-kb recombined allele. (D) PCR analysis of tamoxifen-induced recombination of $Akt^{Ind.Tg}$ allele. Specific oligonucleotides were used to amplify the 473-bp PCR product from the $Akt^{Ind.Tg}$ targeted allele and the 253-bp band from the recombined locus (arrows). DNA recombination of the $Akt^{Ind.Tg}$ cassette is evident only in DNA from muscle (and not in genomic DNA obtained from tails) that has been treated with tamoxifen. (E) Tamoxifen-induced hypertrophy in the $Akt^{Ind.Tg}$ mice. Photographs of skinned WT and $Akt^{Ind.Tg}$ mice obtained 1 week after daily injection with tamoxifen (Tam) for 14 consecutive days. The induced $Akt^{Ind.Tg}$ mice displayed a noticeable size difference in all skeletal muscles. (F) Tamoxifen-dependent gain in $Akt^{Ind.Tg}$ muscle weights. Muscle weights from GA muscles were taken from either untreated (−Tam) or tamoxifen-treated (+Tam) WT and $Akt^{Ind.Tg}$ mice. A significant increase in muscle weight was observed only in the Tam-treated $Akt^{Ind.Tg}$ animal in both males and females. An asterisk indicates a significant difference in $Akt^{Ind.Tg}$ weights compared to all of other control groups ($P < 0.0001$). The mean ± the standard error of the mean is given for each group.

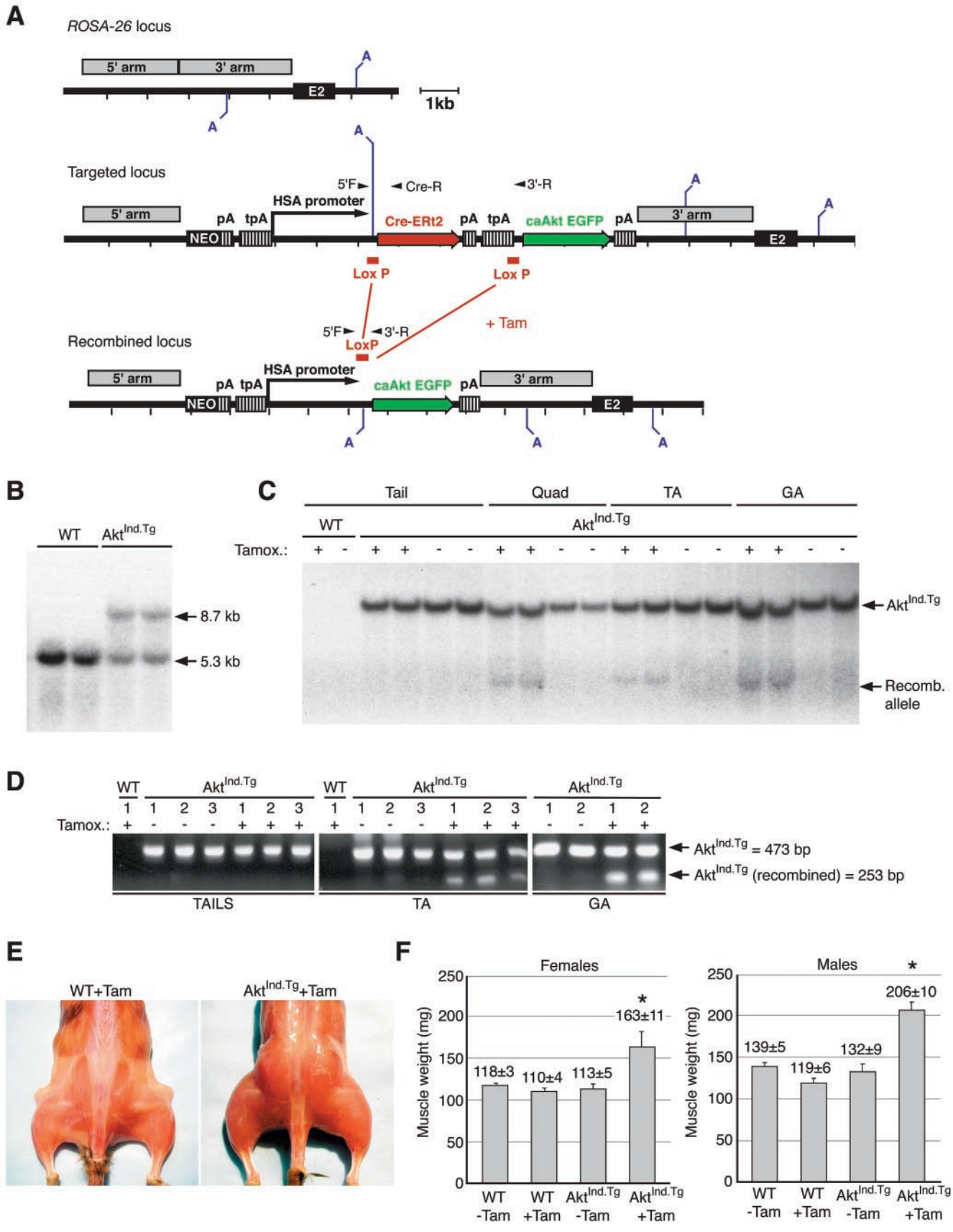
A
ROSA-26 locus
5' arm
3' arm
E2
A
1kb
Targeted locus
5'F
Cre-R
3'-R
HSA promoter
pA tpA
Cre-ERt2
caAkt EGFP
NEO
Lox P
Recombined locus
LoxP
+ Tam
B
WT
Akt Ind.Tg
8.7 kb
5.3 kb
C
Tail
Quad
TA
GA
Tamox.:
Recomb. allele
D
TAILS
TA
GA
Akt Ind.Tg = 473 bp
Akt Ind.Tg (recombined) = 253 bp
E
WT+Tam
Akt Ind.Tg +Tam
F
Females
Males
Muscle weight (mg)
118±3
110±4
113±5
163±11
139±5
119±6
132±9
206±10
WT -Tam
WT +Tam
Akt Ind.Tg -Tam
Akt Ind.Tg +Tam

$Akt^{Ind.Tg}$ animals after tamoxifen treatment, single muscle fibers were imaged by green fluorescence confocal microscopy. Tamoxifen-induced $Akt^{Ind.Tg}$ fibers could be easily identified on the basis of EGFP expression (Fig. 3A). In order to visualize the morphology of the myofibers, immunohistochemistry was performed with an antibody specific for alpha-actinin, which is bound to the Z-line of the sarcomere. This analysis demonstrated that the fibers were patent, with normal organization of the contractile apparatus (Fig. 3B).

We next sought to determine whether the tamoxifen-induced increase in mass was reflected in an increase in individual fiber diameter. Immunohistochemistry was performed on skeletal muscle cross-sections obtained from $Akt^{Ind.Tg}$ muscle treated with tamoxifen and, as negative controls, WT muscle treated with tamoxifen and $Akt^{Ind.Tg}$ muscle treated with oil, which was used as a carrier for the tamoxifen. Fiber diameters outlined by immunohistochemical staining with laminin demonstrated that a majority of the muscle fibers from tamoxifen-treated $Akt^{Ind.Tg}$ animals were hypertrophic (Fig. 3C). These fibers correlated with positive staining for EGFP (Fig. 3C). Muscle fibers expressing c.a.Akt.EGFP appeared normal, with no central nuclei (Fig. 3C and by hematoxylin and eosin staining [data not shown]). Analysis of the plantaris muscle of these cross-sections showed no indication of a change in the number of muscle fibers (data not shown). Muscle fiber size was also determined, and the results showed a significant increase in mean fiber diameter of the tamoxifen-treated $Akt^{Ind.Tg}$ muscle compared to all controls examined (Fig. 3D). This observation is further illustrated in a histogram distribution curve which demonstrated a significant shift in the distribution, with far more larger fibers seen in $Akt^{Ind.Tg}$ (+) tamoxifen (Fig. 3F, fibers ranged from 618 to 6,000 μm^2 in $Akt^{Ind.Tg}$ [−Tam] muscle in size compared to 433 to 19,423 μm^2 in $Akt^{Ind.Tg}$ [+Tam] muscle fibers). Thus, the amount of tamoxifen-induced recombination achieved was sufficient to induce a significant phenotype. There were some larger-than-normal fibers evident in $Akt^{Ind.Tg}$ muscle in the absence of tamoxifen, although the difference was not statistically significant, indicating that there may be some leakiness of expression (Fig. 3E, which is also consistent with the Northern mRNA analysis [Fig. 4A]).

Northern mRNA analysis was performed in order to assess the amount of *c.a.Akt-EGFP* mRNA, which was induced after treatment of $Akt^{Ind.Tg}$ animals with tamoxifen. Comparison of $Akt^{Ind.Tg}$ animals with or without tamoxifen indicated a low but demonstrable level of expression of the *c.a.Akt-EGFP* transgene without tamoxifen treatment, constituting some "leakiness" of the system (Fig. 4A, lanes 1 to 3). This perhaps explains the few larger-than-normal muscle fibers seen in these mice (Fig. 3E). After treatment with tamoxifen, however, there was a significant increase in the amount of *c.a.Akt-EGFP* mRNA expression (Fig. 4A). This increase in *c.a.Akt-EGFP* mRNA corresponded to a robust induction of caAkt-EGFP protein (Fig. 4B, compare levels of endogenous and transgenic Akt-EGFP proteins), which was prominent by 7 days after tamoxifen induction, and increased by 14 and 21 days postinduction (Fig. 4B). The c.a.Akt-EGFP protein was active, as demonstrated with the phospho-specific $Akt^{Ser\text{-}473}$ antibody (Fig. 4B). Furthermore, activated Akt was induced only in $Akt^{Ind.Tg}$ skeletal muscle and not liver, which was taken as a negative control (Fig. 4C).

Finally, to determine whether the c.a.Akt-EGFP was signaling along established Akt pathways, the activation of endogenous p70S6K was assessed (Fig. 4D). Using a phospho-specific antibody that recognizes the activated form of p70S6K, both skeletal muscle from the $Akt^{Ind.Tg}$ treated with tamoxifen and, as a positive control, muscle obtained from WT animals undergoing hypertrophy were demonstrated to have activated p70S6K, as opposed to unperturbed WT muscle or $Akt^{Ind.Tg}$ that was not treated (Fig. 4D). We had previously demonstrated that the Akt/mTOR/p70S6K protein synthesis pathway is a significant mediator of skeletal muscle hypertrophy (2, 18). Thus, enzymatically active, inducible Akt is promoting muscle hypertrophy via the protein synthesis pathways previously identified as mediating this phenotype.

DISCUSSION

In this study two different approaches were used to generate transgenic mice in order to test the effect of Akt activation on skeletal muscle. In the first case, a single copy of a constitutively active form of Akt was expressed in Akt^{Tg} skeletal muscle as a result of recombination into the *ROSA-26* locus. Chimeric expression was sufficient to induce significant hypertrophy. Akt^{Tg} chimeras not only had muscles that were two- to threefold greater in mass than those observed in their WT littermates, they also had little or no adipose tissue, perhaps as a result of the large caloric requirements of their lean body mass. Histological analysis of the chimeric c.a.Akt trans-

FIG. 3. Analysis of skeletal muscle fibers from $Akt^{Ind.Tg}$ animals. (A) Comparison of teased muscle fibers by fluorescent confocal microscopy. A high level of EGFP is consistently correlated to enlarged muscle fibers isolated from the quadriceps muscles of tamoxifen-treated $Akt^{Ind.Tg}$ mice ($Akt^{Ind.Tg}$ + Tam). EGFP fluorescence is not observed in tamoxifen-treated WT (WT+Tam) mice. (B) Immunohistochemical analysis of teased muscle fibers by confocal microscopic imaging. An antibody-specific to alpha-actinin (α-actinin) demonstrates that the hypertrophic fibers isolated from the quadriceps muscle of $Akt^{Ind.Tg}$ mice ($Akt^{Ind.Tg}$+Tam, right panels) maintain structural integrity, as also observed in the WT (WT+Tam, left panels). (C) Immunostaining of skeletal muscle cross-sections obtained from tamoxifen-treated WT (WT+Tam), tamoxifen-treated $Akt^{Ind.Tg}$ ($Akt^{Ind.Tg}$+Tam), and oil-injected $Akt^{Ind.Tg}$ ($Akt^{Ind.Tg}$+Oil) mice. Anti-laminin antibody (top panels in green) and anti-EGFP antibody (middle panels in red) were utilized to outline the borders of muscle fibers and to detect c.a.Akt.EGFP expressing fibers of the GA muscles, respectively. Overlapped images of the sections demonstrated a strong correlation between enlarged fibers (outlines in green) and c.a.Akt.EGFP-positive fibers (red), which were only observed in the cross-sections obtained from $Akt^{Ind.Tg}$+Tam muscles. (D) Mean cross-sectional area of muscle fibers. GA muscle fibers obtained from the tamoxifen-treated $Akt^{Ind.Tg}$ mice ($Akt^{Ind.Tg}$+Tam) have a larger mean area compared to WT muscle or uninduced $Akt^{Ind.Tg}$ muscle. An asterisk indicates a statistically significant difference in $Akt^{Ind.Tg}$ fiber size compared to each of the control groups ($P < 0.0001$). (E) Analysis of fiber size distribution of uninduced WT and $Akt^{Ind.Tg}$ mice. Individual plantaris muscle fibers from uninduced $Akt^{Ind.Tg}$ ($Akt^{Ind.Tg}$−Tam) mice (red bars) were similar in size to fibers from untreated WT (WT−Tam) animals. (F) Distribution of muscle fiber size of $Akt^{Ind.Tg}$ mice with or without tamoxifen. Tamoxifen induces (+Tam) a dramatic increase in $Akt^{Ind.Tg}$ muscle fiber size and significantly shifts the frequency distribution curve to the right (green bars) in comparison to the distribution displayed by the uninduced $Akt^{Ind.Tg}$ muscles (red bars).

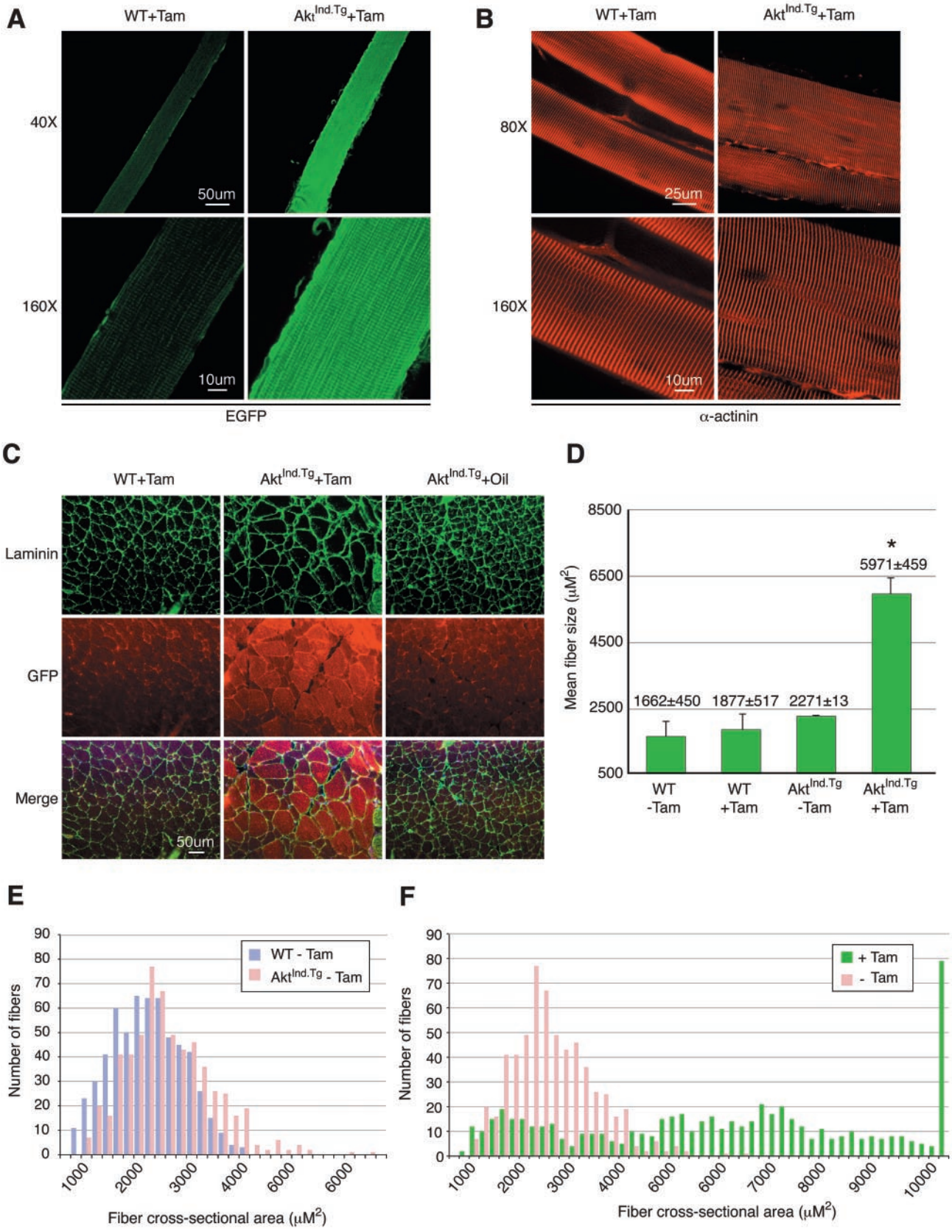
A
WT+Tam
Akt Ind.Tg +Tam
40X
50um
160X
10um
EGFP
B
WT+Tam
Akt Ind.Tg +Tam
80X
25um
160X
10um
α-actinin
C
WT+Tam
Akt Ind.Tg +Tam
Akt Ind.Tg +Oil
Laminin
GFP
Merge
50um
D
Mean fiber size (μM2)
8500
6500
4500
2500
500
*
5971±459
1662±450
1877±517
2271±13
WT -Tam
WT +Tam
Akt Ind.Tg -Tam
Akt Ind.Tg +Tam
E
Number of fibers
WT - Tam
Akt Ind.Tg - Tam
Fiber cross-sectional area (μM2)
F
Number of fibers
+ Tam
- Tam
Fiber cross-sectional area (μM2)

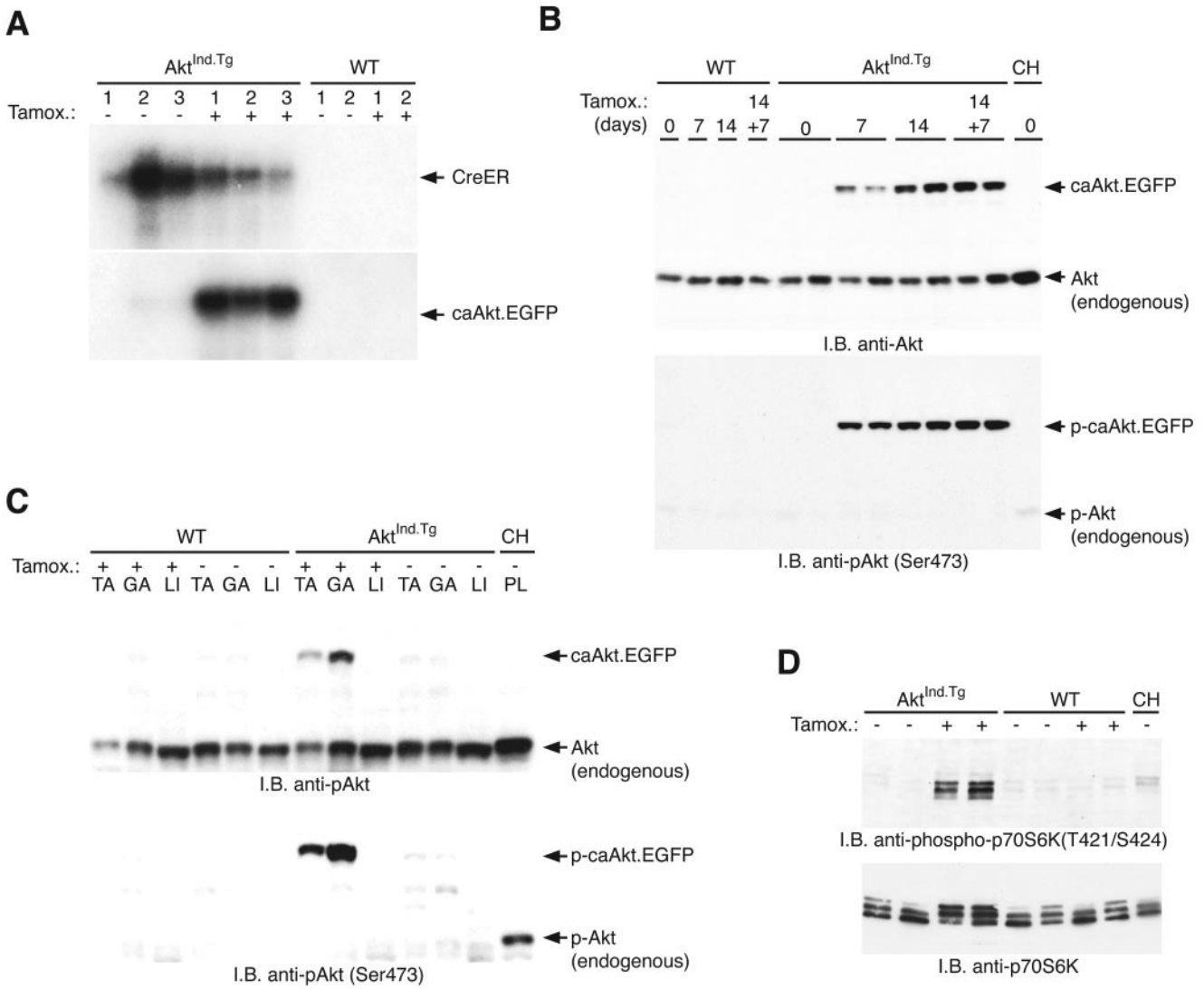

FIG. 4. Tamoxifen-induced c.a.Akt-EGFP transgene expression and biochemistry. (A) Northern analysis of total RNA isolated from control (−) or tamoxifen-treated (+) WT and $Akt^{Ind.Tg}$ quadriceps muscles. The *c.a.Akt-EGFP* transcript was barely detectable in two of the untreated muscle samples (lanes 2 and 3), whereas a high level of the *c.a.Akt-EGFP* transcript was observed after tamoxifen treatment (the arrow points to the single 3-kb band that corresponds to the *c.a.Akt-EGFP* transcript). (B) The transgenic c.a.Akt-EGFP fusion protein is rapidly produced and phosphorylated upon induction with tamoxifen. Tamoxifen-induced c.a.Akt-EGFP expression is prominent by 7 days of tamoxifen treatment in the $Akt^{Ind.Tg}$ quadriceps muscles (top panel, 7 days). The protein level is further induced after 14 days of treatment (top panel, 14 days), and the $Akt^{Ind.Tg}$ locus continues to express the c.a.Akt-EGFP protein 7 days after tamoxifen treatment was halted (top panel, 14 + 7 days). This protein is undetectable in both the untreated $Akt^{Ind.Tg}$ (day 0) and WT mice (top panel, lanes 1 to 4). Comparable amount of endogenous Akt is detected in all muscles (top panel). The induced c.a.Akt-EGFP protein is phosphorylated on serine-473. In the WT animal, only muscle obtained from a CH model is phosphorylated (bottom panel). (C) The transgenic Akt-EGFP fusion protein is produced only in skeletal muscle, as shown by Western immunoblot analysis. Upon treatment with tamoxifen, the c.a.Akt-EGFP fusion protein is evident in TA and GA muscles from the $Akt^{Ind.Tg}$ mice but not in WT muscle. The c.a.Akt-EGFP fusion protein is not evident in liver (LI) even after tamoxifen treatment. Endogenous Akt is seen in muscle from both WT and $Akt^{Ind.Tg}$ animals (compare top panel). Upon treatment with tamoxifen, the induced c.a.Akt-EGFP protein is phosphorylated on serine-473. In the WT animal, only plantaris muscle (PL) obtained from a CH model is phosphorylated (bottom panel). (D) Induction of the transgenic Akt-EGFP fusion protein leads to the activation of endogenous p70S6 kinase. Equal amounts of protein extracts from treated (+) or control (−) $Akt^{Ind.Tg}$ and WT quadriceps muscles were immunoblotted. A phospho-specific antibody for p70S6K demonstrates that p70S6 kinase is only activated in tamoxifen-treated $Akt^{Ind.Tg}$ muscles (top panel). Activation of p70S6 kinase was also visualized by monitoring the total p70S6K protein in a gel shift assay; the upper bands are the phosphorylated, activated form of the protein (bottom panel).

genic animals revealed increased muscle fiber size, demonstrating the phenotype was actual hypertrophy. Biochemical analysis of the transgenic animals demonstrated that the transgenic c.a.Akt-EGFP protein was phosphorylated and therefore biologically active.

The advantages of the approach used to generate Akt^{Tg} animals include high-efficiency recombination into the *ROSA-26* locus and the production of mice with a single copy of the transgene to reduce potential artifacts caused by overexpression. It is noteworthy that tissue-specific expression was achieved by inserting the HSA promoter into the *ROSA-26* locus. Other researchers have used the *ROSA-26* locus to drive

ubiquitous expression, taking advantage of the endogenous *ROSA-26* promoter. The present study establishes that one can also utilize the *ROSA-26* locus to drive tissue specific expression, as long as the appropriate promoter is provided. An additional advantage of generating transgenic mice by gene targeting is that positional effects are avoided by precisely inserting a gene of interest at a known site, achieving consistent and reliable transgenic expression. In this manner, one avoids screening many founder mice as is necessary using conventional transgenic techniques. Although tissue-specific expression was achieved with this approach, the HSA promoter caused a significant amount of embryonic cardiac expression in most of the chimeras analyzed, giving impetus to engineering a transgenic where expression could be induced in the adult animal.

Therefore, a second type of transgenic animal was engineered, in which in a defined locus a single copy of the transgene could be conditionally expressed via tamoxifen-induced autoexcision of the CreERt2 recombinase. With this strategy, the integration site is known, and there is only one copy of the transgene. Also, upon recombination the CreERt2 cassette is eliminated. Further, with this type of transgenic approach the possibility of developmental changes caused by embryonic expression of an active transgene is eliminated by waiting until the animals reached adulthood before induction of the transgene.

Three weeks after tamoxifen-induced expression of the c.a.Akt-EGFP transgene was initiated, several parameters of hypertrophy were apparent. First, skeletal muscle mass was increased approximately twofold. Second, the diameters of individual muscle fibers were shown to be enhanced, again by >2-fold in most of the affected fibers (fibers that underwent activation could be determined by coexpression of the EGFP marker). Third, a dramatic increase in activated Akt protein was detected: Akt activation had previously been established as a marker of hypertrophy. Fourth, the downstream protein synthesis mediator, p70S6K, which is part of the Akt/mTOR/p70S6K pathway, was shown to be activated, which demonstrates that activation of Akt is sufficient to induce activation of p70S6K. Thus, relatively short-term activation of Akt in skeletal muscle is sufficient to induce hypertrophy via induction of protein synthesis pathways.

These data are consistent with a recent report demonstrating that genetic disruption of Akt leads to impairment in organ growth (3) and a report indicating that disruption of both Akt and the related gene Akt2 leads to skeletal muscle atrophy, in addition to other sequelae (17). Thus, it is now clear that the presence of Akt is both necessary to maintain normal skeletal muscle mass and that activation of Akt is sufficient to induce skeletal muscle hypertrophy.

Other mouse models expressing c.a.Akt have been produced. Perhaps the most relevant transgenic model is a mouse in which c.a.Akt was overexpressed in cardiac muscle (21). Expression of c.a.Akt in the heart induced cardiac muscle hypertrophy (21). However, signaling in cardiac muscle is not always predictive of skeletal muscle. For example, overexpression of an active form of the phosphatase calcineurin in cardiac muscle results in significant hypertrophy (12), whereas even 10-fold overexpression of calcineurin in skeletal muscle does not induce hypertrophy (15). Therefore, we establish here that, in contrast to calcineurin, Akt signaling results in hypertrophy in multiple tissue types. These data in combination with the knockout results indicate that Akt may be a "master regulator" of growth, not only because it is required for the maintenance of cell size but also because its activation seems sufficient to increase cell size.

The $Akt^{Ind.Tg}$ transgenic animal serves as a useful genetic model for skeletal muscle hypertrophy and validates the Akt pathway as a target for acute pharmacologic activation in disease settings in which induction of hypertrophy would be useful. Furthermore, the approach used to generate the $Akt^{Ind.Tg}$ transgenic animal represents a step forward in producing genetic models that might accurately mimic the effects of acute pharmacologic activation of protein targets. The production of mouse models that accurately predict the utility of a potential therapeutic target is of considerable importance for pharmaceutical development. Also, as transgenic and knockout technology is becoming more refined, unintended consequences produced through random and multiple genetic integrations can be eliminated, further increasing the value of these models.

ACKNOWLEDGMENTS

We thank L. S. Schleifer and P. R. Vagelos for enthusiastic support, along with the rest of the Regeneron community, and are greatly indebted to our coworkers at Procter and Gamble Pharmaceuticals for their continued support. We thank Esther Latres for helpful discussions. We also thank V. Lan and B. Ephraim for expert graphics work.

REFERENCES

1. **Bodine, S. C., E. Latres, S. Baumhueter, V. K. Lai, L. Nunez, B. A. Clarke, W. T. Poueymirou, F. J. Panaro, E. Na, K. Dharmarajan, Z. Q. Pan, D. M. Valenzuela, T. M. DeChiara, T. N. Stitt, G. D. Yancopoulos, and D. J. Glass.** 2001. Identification of ubiquitin ligases required for skeletal muscle atrophy. Science **294:**1704–1708.
2. **Bodine, S. C., T. N. Stitt, M. Gonzalez, W. O. Kline, G. L. Stover, R. Bauerlein, E. Zlotchenko, A. Scrimgeour, J. C. Lawrence, D. J. Glass, and G. D. Yancopoulos.** 2001. Akt/mTOR pathway is a crucial regulator of skeletal muscle hypertrophy and can prevent muscle atrophy in vivo. Nat. Cell Biol. **3:**1014–1019.
3. **Chen, W. S., P. Z. Xu, K. Gottlob, M. L. Chen, K. Sokol, T. Shiyanova, I. Roninson, W. Weng, R. Suzuki, K. Tobe, T. Kadowaki, and N. Hay.** 2001. Growth retardation and increased apoptosis in mice with homozygous disruption of the Akt1 gene. Genes Dev. **15:**2203–2208.
4. **Coleman, M. E., F. DeMayo, K. C. Yin, H. M. Lee, R. Geske, C. Montgomery, and R. J. Schwartz.** 1995. Myogenic vector expression of insulin-like growth factor I stimulates muscle cell differentiation and myofiber hypertrophy in transgenic mice. J. Biol. Chem. **270:**12109–12116.
5. **Cross, D. A., D. R. Alessi, P. Cohen, M. Andjelkovich, and B. A. Hemmings.** 1995. Inhibition of glycogen synthase kinase-3 by insulin mediated by protein kinase B. Nature **378:**785–789.
6. **Datta, S. R., A. Brunet, and M. E. Greenberg.** 1999. Cellular survival: a play in three Akts. Genes Dev. **13:**2905–2927.
7. **DeVol, D. L., P. Rotwein, J. L. Sadow, J. Novakofski, and P. J. Bechtel.** 1990. Activation of insulin-like growth factor gene expression during work-induced skeletal muscle growth. Am. J. Physiol. **259:**E89–E95.
8. **Feil, R., J. Wagner, D. Metzger, and P. Chambon.** 1997. Regulation of Cre recombinase activity by mutated estrogen receptor ligand-binding domains. Biochem. Biophys. Res. Commun. **237:**752–757.
9. **Florini, J. R., D. Z. Ewton, and S. A. Coolican.** 1996. Growth hormone and the insulin-like growth factor system in myogenesis. Endocrinol. Rev. **17:**481–517.
10. **Glass, D. J.** 2003. Signalling pathways that mediate skeletal muscle hypertrophy and atrophy. Nat. Cell Biol. **5:**87–90.
11. **Goldspink, D. F., P. J. Garlick, and M. A. McNurlan.** 1983. Protein turnover measured in vivo and in vitro in muscles undergoing compensatory growth and subsequent denervation atrophy. Biochem. J. **210:**89–98.
12. **Molkentin, J. D., J. R. Lu, C. L. Antos, B. Markham, J. Richardson, J. Robbins, S. R. Grant, and E. N. Olson.** 1998. A calcineurin-dependent transcriptional pathway for cardiac hypertrophy. Cell **93:**215–228.
13. **Musaro, A., K. McCullagh, A. Paul, L. Houghton, G. Dobrowolny, M. Molinaro, E. R. Barton, H. L. Sweeney, and N. Rosenthal.** 2001. Localized Igf-1 transgene expression sustains hypertrophy and regeneration in senescent skeletal muscle. Nat. Genet. **27:**195–200.

14. **Nave, B. T., M. Ouwens, D. J. Withers, D. R. Alessi, and P. R. Shepherd.** 1999. Mammalian target of rapamycin is a direct target for protein kinase B: identification of a convergence point for opposing effects of insulin and amino-acid deficiency on protein translation. Biochem. J. **344**(Pt. 2)**:**427–431.
15. **Naya, F. J., B. Mercer, J. Shelton, J. A. Richardson, R. S. Williams, and E. N. Olson.** 2000. Stimulation of slow skeletal muscle fiber gene expression by calcineurin in vivo. J. Biol. Chem. **275:**4545–4548.
16. **Pallafacchina, G., E. Calabria, A. L. Serrano, J. M. Kalhovde, and S. Schiaffino.** 2002. A protein kinase B-dependent and rapamycin-sensitive pathway controls skeletal muscle growth but not fiber type specification. Proc. Natl. Acad. Sci. USA **25:**25.
17. **Peng, X. D., P. Z. Xu, M. L. Chen, A. Hahn-Windgassen, J. Skeen, J. Jacobs, D. Sundararajan, W. S. Chen, S. E. Crawford, K. G. Coleman, and N. Hay.** 2003. Dwarfism, impaired skin development, skeletal muscle atrophy, delayed bone development, and impeded adipogenesis in mice lacking Akt1 and Akt2. Genes Dev. **17:**1352–1365.

17a. **Ralston, E., and T. Plong.** 1996. Pre-embedding staining of single muscle fibers for light and electron microscopy studies of subcellular organization. Scanning Microsc. Suppl. **10:**249–259.

18. **Rommel, C., S. C. Bodine, B. A. Clarke, R. Rossman, L. Nunez, T. N. Stitt, G. D. Yancopoulos, and D. J. Glass.** 2001. Mediation of IGF-1-induced skeletal myotube hypertrophy by PI(3)K/Akt/mTOR and PI(3)K/Akt/GSK3 pathways. Nat. Cell Biol. **3:**1009–1013.
19. **Rommel, C., B. A. Clarke, S. Zimmermann, L. Nunez, R. Rossman, K. Reid, K. Moelling, G. D. Yancopoulos, and D. J. Glass.** 1999. Differentiation stage-specific inhibition of the raf-MEK-ERK pathway by Akt. Science **286:** 1738–1741.
20. **Scott, P. H., and J. C. Lawrence, Jr.** 1998. Attenuation of mammalian target of rapamycin activity by increased cAMP in 3T3-L1 adipocytes. J. Biol. Chem. **273:**34496–34501.
21. **Shioi, T., J. R. McMullen, P. M. Kang, P. S. Douglas, T. Obata, T. F. Franke, L. C. Cantley, and S. Izumo.** 2002. Akt/protein kinase B promotes organ growth in transgenic mice. Mol. Cell. Biol. **22:**2799–2809.
22. **Valenzuela, D., A. Murphy, D. Frendewey, N. Gale, A. Economides, W. Auerbach, W. Poueymirou, N. Adams, J. Rojas, J. Yasenchak, R. Chernomorsky, M. Boucher, A. Elsasser, L. Esau, J. Zheng, J. Griffiths, X. Wang, H. Su, Y. Xue, M. Dominguez, I. Noguera, R. Torres, L. MacDonald, A. Stewart, T. DeChiara, and G. Yancopoulos.** 2003. High-throughput engineering of the mouse genome coupled with high-resolution expression analysis. Nat. Biotechnol. **21:**652–659.
23. **Vivanco, I., and C. L. Sawyers.** 2002. The phosphatidylinositol 3-kinase AKT pathway in human cancer. Nat. Rev. Cancer **2:**489–501.
24. **Zambrowicz, B. P., A. Imamoto, S. Fiering, L. A. Herzenberg, W. G. Kerr, and P. Soriano.** 1997. Disruption of overlapping transcripts in the ROSA beta geo 26 gene trap strain leads to widespread expression of β-galactosidase in mouse embryos and hematopoietic cells. Proc. Natl. Acad. Sci. USA **94:**3789–3794.